Iranian Journal of Science & Technology, Transaction B, Engineering, Vol. 34, No. B1, pp 35-48
Printed in The Islamic Republic of Iran, 2010


# EXPERIMENTAL AND ANALYTICAL STUDY ON BEHAVIOUR OF CFRP-STRENGTHENED HSC BEAMS WITH MINIMUM REINFORCEMENT UNDER PURE TORSION*

M. R. MOHAMMADIZADEH[1**] AND M. J. FADAEE[2]

[1]Dept. of Civil Engineering, Hormozgan University, Bandar Abbas, I. R. of Iran
[2]Dept. of Civil Engineering, Kerman University, Kerman, I. R. of Iran
Email: mrzmohammadizadeh@yahoo.com

**Abstract–** Experimental investigation was conducted to study the pure torsional behaviour of high-strength concrete (HSC) beams strengthened with carbon-fibre-reinforced-polymers (CFRP) having minimum torsional reinforcement. A total of six beams were tested. Two beams without CFRP were assigned as control beams and the rest were strengthened using CFRP sheets. In this study, different wrap configurations, the effect of different numbers of CFRP plies, and the influence of anchors in U-wrapped test beams considered as variables were investigated. Investigation into ductility using two different concepts showed enhancement in the behaviour of strengthened beams with CFRP. The ductility of the beam strengthened with two complete CFRP layers was fifty percent higher than that of the control beams. The beam strengthened using this scheme showed a 75% increase in torsional capacity compared to the control beam, which was not strengthened. The experimental results were compared with the results from three analytical methods. The ultimate torsional strength resulting from one of the three methods, which was based upon synthesis of an analytical method and average CFRP strains obtained from experiments, was in good agreement with the experimental results.
.

**Keywords–** Analytical, carbon-fibre-reinforced-polymers (CFRP), high-strength concrete (HSC), ductility, minimum reinforcement, strengthening, torsion

## 1. INTRODUCTION

### *a) The importance of using composite materials in strengthening*

Deterioration of reinforced concrete structures, due either to corrosion of the reinforcement bars or to the continual upgrading of service loads (for example, increase in the traffic load on a bridge) has resulted in a large number of structures requiring repairing or strengthening.

Various methods are available to repair or strengthen such structures. External bonding of composite materials to deficient or damaged reinforced concrete structures is one type of strengthening method. Because CFRP materials are non-corrosive, non-magnetic, resistant to various types of chemicals, high in strength, and lightweight, they are increasingly being used for external reinforcement of existing concrete structures.

There is limited information [1-14] on strengthening torsional members with fibre-reinforced-polymers (FRP) in the literature and all of them have been carried out on torsional strengthening of normal strength concrete beams. Therefore, practically no work has yet been carried out concerning torsional repair of high-strength concrete beams. The lack of experimental and analytical studies in this field led to the present study on the torsional behaviour of reinforced concrete beams repaired with CFRP sheets.

*Received by the editors June 23, 2008; Accepted October 27, 2009.
**Corresponding author

***b) Simulation of deficient beams because of corroded bars by providing minimum torsional reinforcement***

In the present investigation, a minimum amount of torsional reinforcement has been used in the specimens in order to model a beam with corroded reinforcement. The minimum value is defined so that it prevents premature failures immediately after inclined cracking occurs. In ACI 318-05, the minimum torsional reinforcement required for reinforced concrete (RC) beams made of concrete with compressive strength up to $69\,MPa$ is specified to be equal to 1% [15].

Koutchoukai and Belarbi investigated the effect of high-strength concrete on the torsional cracking strength [16]. Their experimental results showed that the minimum amount of torsional reinforcement recommended in ACI 318-95 was inadequate for high-strength RC beams. They concluded that for avoiding brittle failure (at the onset of cracking), 20% of strength must be reserved after cracking for the beam to experience uniform cracks along its length. Based upon this conclusion, they developed a new expression for minimum torsional reinforcement in terms of the concrete compressive strength. The new expression for providing minimum torsional reinforcement is based upon the yield strength of the transverse and longitudinal reinforcement and concrete compressive strength.

## 2. EXPERIMENTAL PROGRAM

***a) Specimens' details***

A total of six beams were cast and cured under laboratory conditions in this experimental investigation. The beams had the same size and steel reinforcement. All beams were $2000\,mm$ long, having a cross-section of $150\times350\,mm$ with a concrete cover of $25\,mm$. To force failure in the central region of the test beam, hereafter referred to as "test region", stirrup spacing at the ends of the beam was reduced to almost half of the stirrup spacing at the centre. The length of the test region of the specimens was approximately $1600\,mm$. The reinforcement layout was designed for minimum torsional capacity to simulate a torsionally deficient beam because of extensively corroded bars. Therefore, the transverse and longitudinal reinforcements were arranged according to the design provisions of ACI 318-05 [15] and reference [16]. Longitudinal reinforcement consisted of four bars with $10\,mm$ diameters, one at each corner of the cross-section and stirrups having $8\,mm$ diameters with a spacing of $80\,mm$. The total steel ratio of longitudinal and transverse reinforcement, based upon reserving a minimum of 20% of the strength after cracking, was considered to be equal to $1.56\%$. Two of the beams, called CTRL1 and CTRL2, were tested without CFRP as control beams and the rest were strengthened by carbon fibre (Mbrace CF 240) in different configurations. Properties of the used fibre are stated in Table 1, [17].

Table 1. Properties of the fibres [17]

| Type of fibre | Thickness (mm) | Modulus of elasticity (MPa) | Ultimate tensile strength (MPa) | Ultimate tensile elongation |
|---|---|---|---|---|
| CF 240 | 0.176 | 240,000 | 3800 | 1.55% |

In all strengthened beams, CFRP was used vertically with respect to the longitudinal beam axis. One of the beams, called CW1, was wrapped by one layer of CFRP around the perimeter of the section and along the entire beam. Beam CW2 was wrapped by two layers of CFRP, beam CUJ-anc. was wrapped by CFRP on two sides and also the bottom as a U-jacket along the entire beam, and the free edges of CFRPs on the two sides were fastened to the top of the beam.

Beam CS1 was wrapped using a one-layer $100\,mm$ strip of CFRP around the perimeter of the section, having $100\,mm$ spacing. The overlap length for the CFRP wrap was $15cm$. Table 2 states the specifications of the specimen beams.

Table 2. Summary of specimens' details

| Specimen | Composite sheets | No. of layers | Anchor used | Concrete compressive strength, (MPa) |
|---|---|---|---|---|
| CTRL1 | Control beam | None | - | 78.12 |
| CTRL2 | Control beam | None | - | 80.89 |
| CW1 | Full wrap | 1 | No | 73.18 |
| CW2 | Full wrap | 2 | No | 73.24 |
| CS1 | Full Strip | 1 | No | 74.39 |
| CUJ-anc. | U-jacket | 1 | Yes | 73.67 |

***b) Material properties***

High-strength concrete was designed for a 28-day cylinder compressive strength of $75\,MPa$, and supplied by a local ready-mix plant. The actual concrete strength was considered as the average of at least six standard cube specimens of $100\times100\times100\,mm$ converted to American cylinder specimen strength. The maximum size of coarse aggregate for the concrete was $10\,mm$, and both beams and cubes were kept under the same curing condition until the testing time.

The yield strengths of the transverse and longitudinal reinforcement bars were obtained from tensile tests. These values were $480\,MPa$ and $352\,MPa$ for the transverse and longitudinal reinforcement, respectively.

***c) Test setup and instrumentation***

Details of the setup are shown in Fig. 1. A 2-MN hydraulic jack was used to apply the load at the active support. The load had a $400\,mm$ lever arm from the centroidal axis of the beam. A 2-MN compression load cell was used to measure the applied load. The hydraulic jack had a stroke length of $150\,mm$ providing a 35-degree twist capacity for the beam. A reaction arm was used at the passive support to balance the applied load by attaching the arm to the laboratory strong floor. The reaction arm had a $400\,mm$ eccentricity from the centroidal axis of the beam as well. After cracking, the beam elongated longitudinally. To avoid any longitudinal restraint and subsequent compression, the beam was allowed to slide and elongate freely. This was achieved by supporting the end of the beam on rollers at the passive support. The angle of twist of the free end (the point of applying the torque) was measured by a clinometer.

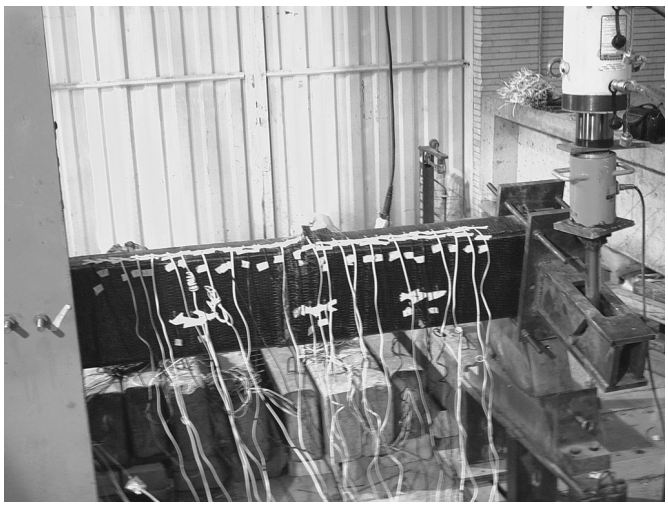

Fig. 1. Test setup

In each beam, 12 electrical resistance strain gauges were used to measure strains on the reinforcing bars. Three strain gauges were mounted on three stirrups within the test region, one stirrup located at mid-span and two stirrups located symmetrically at $400\,mm$ from the mid-span. Each stirrup was instrumented with one strain gauge, mounted at the middle of the long leg (side face; see Fig. 2). Nine strain gauges were mounted on longitudinal bars at three different sections of the test region. One set of three gauges was located in the middle, and the other two sets were symmetrically located at $400\,mm$ from the middle, on each side of the test beam. At each section, two gauges were mounted on the bottom corner bars and one gauge on the upper corner bar.

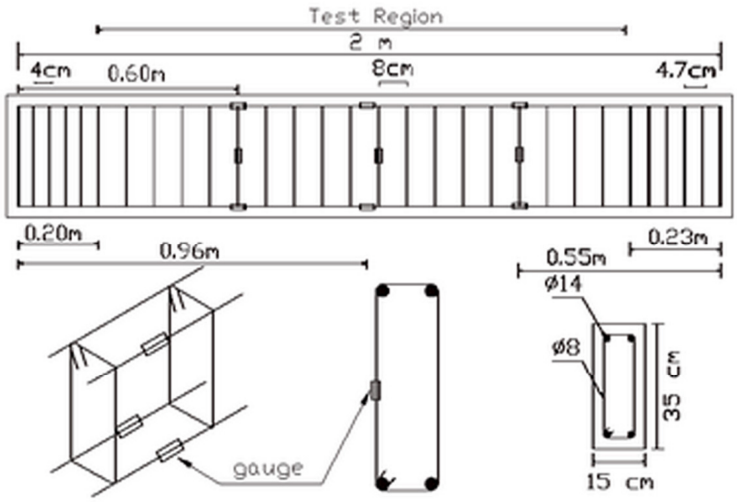


Fig. 2. Location of strain gauges along the beam, strain gauges on stirrups, strain gauges on longitudinal bars

For each strengthened beam, in addition to the instruments provided as for the reference beams, at least 36 strain gauges were also attached to the CFRP sheets on the middle part of one side, along the principal fibre direction with a spacing of $50\,mm$. This high number of strain gauges was used because the failure region along the entire length of the beam under pure torsion was unknown.

***d) Test procedure***

Loads and strain readings were recorded through a computer-driven data acquisition system. Before testing, the cracking and ultimate strengths of the beam specimens were estimated using the available analytical methods. Prior to the failure of the beam, data were recorded at each prescribed load increment. Smaller increments were applied closer to the cracking state to accurately measure the torque value closest to the actual cracking torque. The loading process was carried out as stress control. For the control beams, at every load stage after cracking, the load was held constant for several minutes before recording data, after which the crack pattern was marked and crack width and spacing were measured.

## 3. TEST RESULTS AND DISCUSSIONS

***a) The behaviour of the strengthened beams***

The cracking and yield torques of all strengthened beams are listed in Table 3, indicating their increase percentage compared to the control beams.

Table 3. Cracking and yielding torques obtained from experiments and corresponding increase percentage

| Specimen | Cracking torque (kN.m) | Yield torque (kN.m) | Cracking torque increasing (%) | Yield torque increasing (%) |
|---|---|---|---|---|
| CTRL1 | 10.200 | 13.82 | - | - |
| CTRL2 | 10.200 | 12.82 | - | - |
| CW1 | 13.330 | 17.46 | 30.69 | 31.08 |
| CW2 | 15.150 | 17.63 | 48.53 | 32.36 |
| CS1 | 12.550 | 13.56 | 23.04 | 1.80 |
| CUJ-anc. | 13.500 | 17.31 | 32.35 | 29.95 |

The increase percentage of cracking and yield torques in Table 3 result from comparing the corresponding torques of the beams strengthened by CFRP with the average cracking and yield torque of the control beams (specimens CTRL1 and CTRL2).

Figure 3 shows torque-strain curves for all specimens. The curves in this figure are plotted based on the longitudinal bars' strain.

As the longitudinal reinforcement percentage is lower than the transverse reinforcement percentage in all the specimen beams subjected to the load, the longitudinal bars will yield first, followed by yielding of the transverse bars. Therefore, strains of the longitudinal bars are considered for plotting torque-strain curves.

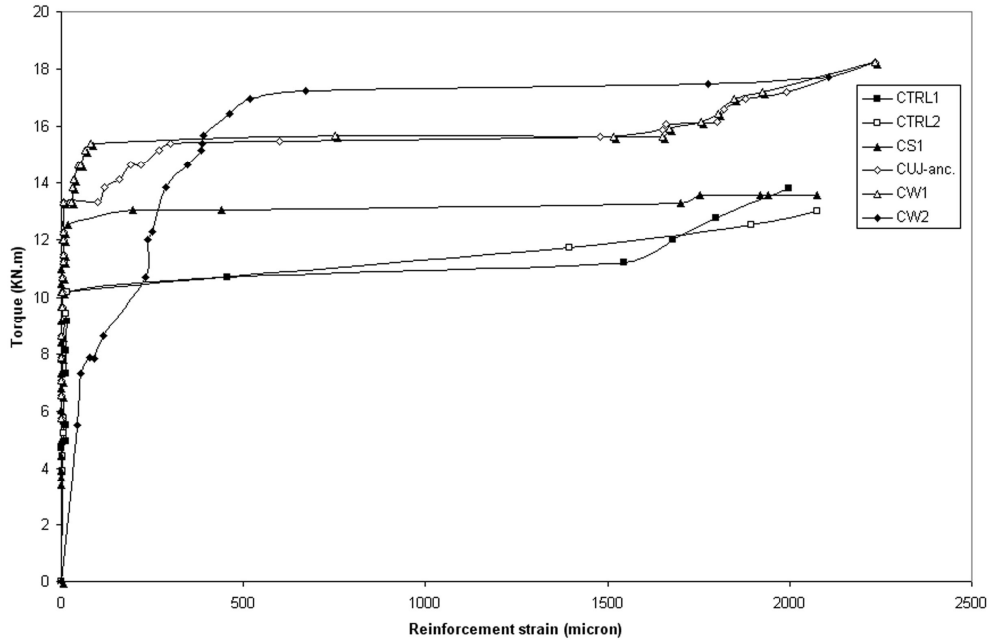


Fig. 3. The strain–torque curves based on the strain in the longitudinal reinforcement bars

Figure 3 shows that the cracking torque values for the two control beams are the same. It can also be seen that the cracking and yield torques of all strengthened beams are greater than those of the control beams. In other words, interaction forces between externally bonded CFRP composites and concrete cause numerous cracks on the beam surfaces, whereas in the beam without CFRP, helical cracks are created with rather larger distances compared to the strengthened beams. In fact, at initial cracking stage, the stresses that are created on the strengthened beams' surfaces are smaller compared to those of the beams without CFRP. This is due to the effect of redistribution of diagonal tensile stresses on the strengthened beam surfaces. Consequently, in the strengthened beams, overall cracking occurs at a higher load level. The increase magnitude depends on the CFRP's reinforcement ratio and the strengthening configuration.

A maximum increase of 48.53% and 32.36% for cracking and yield torque, respectively, were recorded for CW2.

Figure 4 exhibits the crack distribution on one side of the strengthened specimens. The angles of the major cracks in the unwrapped beams were usually around $45^\circ$. The range of the angles for such cracks in the CFRP strengthened beams was $40.5^\circ$ to $49.5^\circ$.

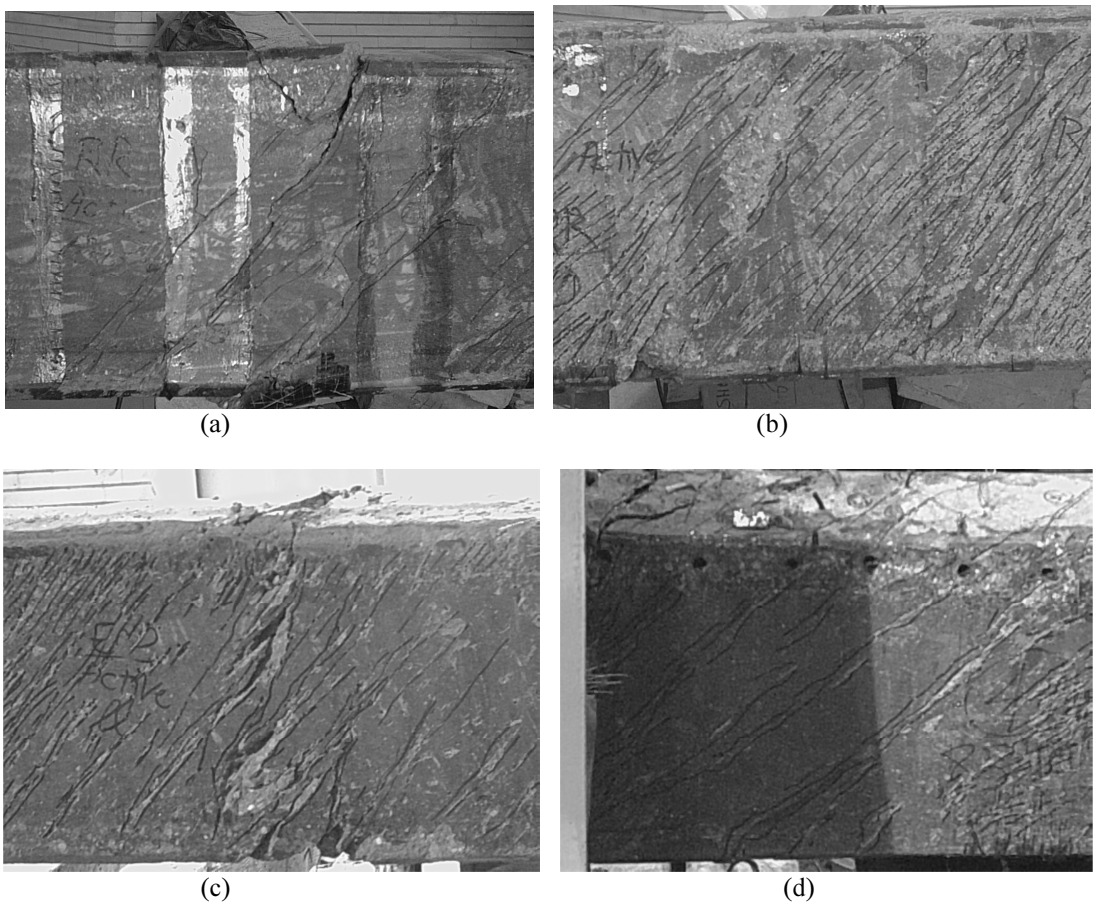

(a) (b) (c) (d)

Fig. 4. The crack distribution in the strengthened specimen beams: a) Specimen CS1; b) Specimen CW1; c) Specimen CW2; d) Specimen CUJ-anc.

Table 4 indicates the results of the tests in terms of the cracking twist angle, $\phi_{cr}$, the ultimate torque, the corresponding torque increase percentage and modes of failure for all six specimens. In Table 4, the increase percentages of the ultimate torques have been computed by comparing the ultimate torques of the beams strengthened by CFRP with the average ultimate torques of the control beams (specimens CTRL1 and CTRL2).

Table 4. Cracking twist angle, ultimate torque and corresponding torque increase percentage of the beams

| Specimen | $\phi_{cr}$ (Degrees) | $T_{n_{\max}}$ (kN.m) | Ultimate torque increasing (%) | Mode of failure |
|---|---|---|---|---|
| CTRL1 | 1.05 | 15.07 | - | Yield & Crushing |
| CTRL2 | 1.50 | 13.75 | - | Yield & Crushing |
| CS1 | 1.30 | 15.83 | 9.88 | Rupture |
| CUJ-anc. | 1.50 | 22.00 | 52.69 | Rupture |
| CW1 | 1.60 | 21.41 | 48.54 | Rupture |
| CW2 | 2.00 | 25.26 | 75.29 | Rupture |

It can be observed in Tables 3 and 4 that the cracking, yield and ultimate torque values of specimens CUJ-anc. and CW1 are approximately the same, in spite of the fact that only three sides of beam CUJ-anc. are strengthened. This may be due to the anchoring influence being much more effective than the strengthening configuration in this case. In fact, the anchors were used to eliminate de-bonding or de-lamination of the CFRP jacket at the free edges. Furthermore, the loop of the force transferring mechanism provided by the composite sheets was completed by the bolts.

The torque-twist behaviour of the beams wrapped with CFRP sheets, along with the control beams are shown in Fig. 5.

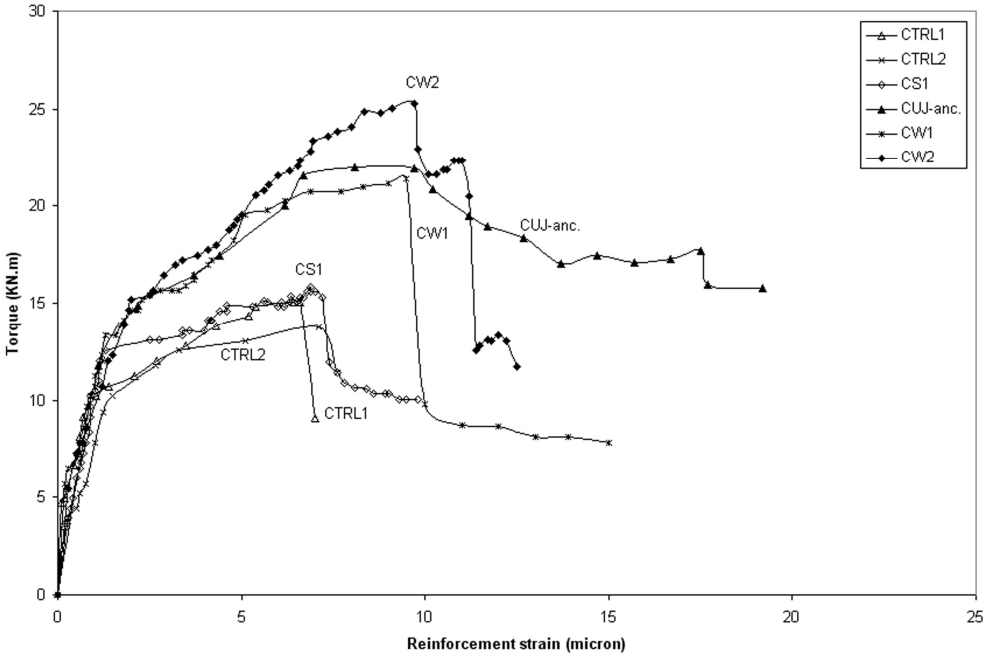


Fig. 5. The behaviour of all the specimen beams based upon experimental torque-twist curves

In Fig. 5, curves are labelled for the code of the specimens. As expected, low difference in the compressive strengths of the control beams does not cause a difference in their behaviour.

It can be observed in Fig. 5 that the behaviour of completely (non-strip) wrapped specimen beams, such as CW1, CUJ-anc. and CW2 is not similar to the behaviour of beam CS1, because the cracks in the completely wrapped beams were not allowed to be widened due to the restraint provided by the fibres. Figure 5 also shows that the beams wrapped completely with CFRP provide much higher ultimate torque compared to the beam strengthened with CFRP strip wrap. The reason for the deficiency in the strengthened beam CS1 using strip in comparison with the full wrapped beams is that the cracks occurred between the strips and then widened.

In Fig. 5, the specimen beams CW1, CUJ-anc. and CW2 exhibit a higher post-cracking stiffness compared to that of specimen beams CTRL1 and CTRL2, and even specimen beam CS1. This is due to the additional reinforcement provided by CFRP fibres. In other words, after cracking, the CFRP reinforcement sustains the applied load along with the steel reinforcement bars.

Qualitatively, there are three different behavioural zones on each torque-twist curve in Fig. 5. The first zone represents the stiffness of the un-cracked beam; the second zone represents the stiffness of the cracked concrete beam strengthened with CFRP sheets; and finally, the third zone corresponds to a damaged beam with wide cracks, yield torsional reinforcement and ruptured composite material.

As indicated in Fig. 6, the failure mode of all the strengthened beams at ultimate torque is controlled by CFRP rupture. This phenomenon is attributed to the configuration of CFRP wrapping in the strengthened beams, which is full (four-side) wrapping.

(a) (b) (c) (d)

Fig. 6. The failure modes of all the strengthened specimen beams: a) Specimen CS1; b) Specimen CW1; c) Specimen CW2; d) Specimen CUJ-anc

In beam CS1, after rupturing the second CFRP strip at the region close to the active support, the cracks of that region will widen causing failure of the beam at a region close to the same support (Fig. 6a).

Beam CW1 reached an ultimate torsional torque of $21.41 KNm$, which was $48.54\%$ more than the average ultimate torque of the control beams. As can be seen in Fig. 4b, after developing cracks in the beam, the CFRP will rupture, followed by extensive concrete cracking, which ultimately results in the beam's failure at a region close to the active support (Fig. 6b).

Beam CW2 bears the highest ultimate torque among all the strengthened beams because of entire beam strengthening and a higher number of CFRP layers. It sustains an ultimate torsional moment 75.29% higher than the average ultimate torque of the control beams. This beam fails through the CFRP rupture at a region close to the active support (Fig. 6c).

The behaviour of beam CUJ-anc. until the ultimate strength point is similar to beam CW1 and it sustains ultimate torque very close to that of CW1. During loading, the cracks created on the top face of the beam (where it is not wrapped by CFRP) gradually widen. The beam fails when the CFRP ruptures at a region near the passive support where one of the cracks becomes the major crack (Fig. 6d).

***b) Ductility***

The ductility ratio, $\mu_\phi$, is usually defined as:

$$\mu_\phi = \frac{\phi_P}{\phi_Y} \tag{1}$$

where $\phi_P$ is the twist angle at the ultimate torque and $\phi_Y$ is the yield twist angle. This ratio indirectly represents the amount of energy that a member can store during plastic deformations, and so represents the

ductility or energy absorbing capacity of the member. This concept of ductility can be applied to strengthened reinforced concrete members in a similar manner.

Some other researchers have proposed the following relation for ductility ratio [18]:

$$\mu_{\phi,0.85P} = \frac{\phi_{0.85P}}{\phi_Y} \tag{2}$$

where $\phi_{0.85P}$ is the twist angle at 85% of the peak torque beyond the peak point.

Ductility ratios are calculated for beams using both Eqs. (1) and (2) and then tabulated in Table 5.

Table 5. Comparison of specimens' ductility ratios based upon $\phi_P$ and $\phi_{0.85P}$

| Specimen | $\phi_y$ | $\phi_P$ | $\mu_{\phi,P} = \phi_P / \phi_y$ | Ductility increasing, Eq.1 (%) | $\phi_{0.85P}$ | $\mu_{\phi,o.85P} = \phi_{0.85P} / \phi_y$ | Ductility increasing, Eq.2 (%) |
|---|---|---|---|---|---|---|---|
| CTRL1 | 4.20 | 6.60 | 1.57 | - | 6.76 | 1.61 | - |
| CTRL2 | 4.36 | 7.10 | 1.63 | - | 7.50 | 1.72 | - |
| CS1 | 4.00 | 6.90 | 1.73 | 8.13 | 7.30 | 1.83 | 9.58 |
| CUJ-anc. | 4.30 | 9.70 | 2.26 | 41.25 | 12.50 | 2.91 | 74.25 |
| CW1 | 4.35 | 9.50 | 2.18 | 36.25 | 9.70 | 2.23 | 33.53 |
| CW2 | 4.00 | 9.70 | 2.44 | 52.50 | 10.10 | 2.53 | 51.50 |

In Table 5, the ductility ratios of the strengthened beams resulting from Eqs. (1) and (2) are compared with the average ductility ratio of the control beams CTRL1 and CTRL2, obtained from the corresponding equations individually.

Maximum ductility ratio, using Eqs. (1) and (2), belongs to beam CW2 with values of 2.44 and 2.53, respectively. These values show an average increase of 52 % in ductility compared to the average ductility of beams CTRL1 and CTRL2. The average least increase percentage in ductility using Eqs. (1) and (2) relates to beam CS1, with values of 8.13% and 9.58%, respectively.

It can be also seen that for all the strengthened beams, except beam CUJ-anc., the ductility increase percentage based upon Eq. (2) is slightly higher than the outcome from Eq. (1).

The ductility increase percentage of beam CUJ-anc. based upon Eq. (2) is the highest value among all the strengthened beams, even beam CW2. This may be due to the lower confinement of beam CUJ-anc. compared to the beams strengthened by complete CFRP wrapping. During loading, the number of cracks created along the entire top face of the beam (where there is no CFRP wrapping) are lower and their width is higher compared to the cracks created on the other three faces of the beam. Unlike those beams that are strengthened along their entire length completely, a sudden decrease in load bearing is not observed at the moment of CFRP rupture. Hence, the load descends evenly.

***c) Experimental data analysis***

Analytical methods for calculating the FRP contribution to the torsional capacity of strengthened beams are very limited. These methods are illustrated briefly in the following.

**1. Analytical method of FIB-14 [19]:** One of the analytical methods appears in FIB-14, and uses the experimental results of the effective strain of beams strengthened in the shear. In FIB-14, the FRP contribution to the torsional capacity due to coupled forces created by a closed tube is considered. In this method, ultimate torque calculations are based upon the fibre orientation and the mode of failure. When the failure of the test beam is controlled by FRP rupture and the fibres' orientation is vertical to the longitudinal axis, the contribution of the FRP sheets to ultimate strength is determined using the effective strain in the fibres. Effective strain in fibres is determined using the empirical equations proposed in FIB -

Technical Report [19]. If the rupture of the fibres does not govern the failure mode, a design approach based upon effective bond length is used to calculate the ultimate strength [20]. Thus, the FRP contribution to the torsional capacity, based on the above mentioned subjects, $T_{n_{frp}}$, is defined by the following relationships:

For complete wrap and strip:

$$T_{n_{frp}} = 2\varepsilon_{ke,f} E_{fu} \frac{t_f b_f}{s_f} A_c \left[\cot\alpha + \cot\beta\right]\sin\beta \tag{3}$$

For U-wrap with anchors:

$$T_{n_{frp}} = \varepsilon_{ke,f} E_{fu} \frac{t_f b_f}{s_f} A_c \left[\cot\alpha + \cot\beta\right]\sin\beta \tag{4}$$

where $E_{fu}$ is the modulus of elasticity of FRP in the principal fibre orientation, $t_f$ is the thickness of the FRP sheet, $s_f$ is the centre-to-centre spacing of FRP strips, $b_f$ is the minimum width of the cross-section over the effective depth of the cross-section (for beams with continuous jacket, the terms $b_f$ and $s_f$ have identical values), $A_c$ is the gross sectional area of the concrete, $P_c$ is the circumference enclosing the gross sectional area of the concrete, $\alpha$ is the angle of torsion crack and $\beta$ is the angle of the orientation of the fibres, both measured from the member's longitudinal axis, and $\varepsilon_{ke,f}$ is the characteristic value of effective fibre strain, defined as:

$$\varepsilon_{ke,f} = K\varepsilon_{f,e} \le \varepsilon_{\max} = 5000\mu \tag{5}$$

where $K$ is the reduction ratio for defining the characteristic effective strain of FRP. The corresponding equation to calculate the effective strain in FRP, $\varepsilon_{f,e}$, is available in reference [19]. In this method, the crack angle, $\alpha$, is assumed to be equal to $45^\circ$.

**2. Hii's method [12]:** The second method was presented by Hii *et al.* [12]. In his proposed method, in order to calculate the FRP contribution to the torsional capacity, the solid section under torsion is considered as an equivalent hollow tube.

For complete wrap and strip:

$$T_{n_{frp}} = 2\varepsilon_{ke,f} E_{fu} \frac{t_f b_f}{s_f} (o.85A_{\circ h}) \left[\cot\alpha + \cot\beta\right]\sin\beta \tag{6}$$

where $A_{\circ h}$ is the area enclosed by the outermost closed stirrups. In this method, the maximum crack angle is considered to be equal to $45^\circ$.

**3. Using FIB-14 method and FRP strain obtained from experiments:** The third method is using FIB-14's equations and the average effective strain obtained from the experiments.

In this method, the crack angle value of $49.5^\circ$ obtained from the experiments is considered for calculating the contribution of the FRP and RC beam without FRP to the torsional strength.

In order to compare the effective strain obtained from the experiments with the calculated effective strain, the calculated effective strain, $\varepsilon_{f,calc}$, for each strengthened specimen is determined from the experimental FRP contribution to torsional torque, $T_{f,\exp}$, by the following equation which results from Eq. (3),

$$\varepsilon_{f,calc} = T_{f,\exp} \Big/ \left[2E_f b_f t_f s_f^{-1} A_c (\cot\alpha + \cot\beta)\sin\beta\right] \tag{7}$$

where the experimental FRP contribution to torsional strength, $T_{f,\exp}$, is determined by subtracting the ultimate torques of the control beams, $T_{ctrl}$, from the ultimate torques of the strengthened specimens, $T_{\exp}$ ($T_{f,\exp} = T_{\exp} - T_{ctrl}$).

Table 6 shows the effective, the characteristic effective, and the average experimental effective strain values. The values in the first, second and the last columns were obtained from FIB-14 and the recorded data at the peak torque, respectively. The average composite tensile strain recorded on the beam side ranged between 1626 to 4754 micro-strain, well below the composite ultimate strain of 1.55%.

Table 6. Comparison of the average experimental effective strain with the effective strain obtained from corresponding equations

| Specimen | $\varepsilon_{f,e}(\mu\varepsilon)$ | $\varepsilon_{ke,f}(\mu\varepsilon)$ | $\varepsilon_{f,calc}(\mu\varepsilon)$ | $\varepsilon_{f,ave,\exp}(\mu\varepsilon)$ |
|---|---|---|---|---|
| CS1 | 11231 | 5000 | 938 | 4754 |
| CUJ-anc. | 9082 | 5000 | 1860 | 3101 |
| CW1 | 8832 | 5000 | 1727 | 2545 |
| CW2 | 7388 | 5000 | 1298 | 1626 |

In this work, three methods were used for calculating the torsional capacity due to the CFRP sheets.

It must be noted that the results of Eq. (3) for specimen CUJ-anc. are very close to the experimental results, but surprisingly, the CFRP contribution to the torsional strength of specimen CUJ-anc. obtained from the experiments is twice the value that resulted from Eq. (4), which is recommended in the literature for such beams. Of course, more experiments are required to confirm this issue.

In Table 7, the values of torsional strength due to CFRP reinforcement obtained from the analytical methods are compared with the experimental values.

Table 7. Comparison of experimental and analytical ultimate torques due to CFRP reinforcement

| Specimen | $T_{f,\exp}/T_{n,frp}$ | $T_{f,\exp}/T_{n,frp}$ | $T_{f,\exp}/T_{n,frp}$ |
|---|---|---|---|
| | FIB-14 | Hii's method | FIB-14 & $\varepsilon_{f,.\ \ ,\exp}(\mu\varepsilon)$ |
| CS1 | 0.13 | 0.29 | 0.18 |
| CUJ-anc. | 0.34 | 0.79 | 0.75 |
| CW1 | 0.32 | 0.73 | 0.85 |
| CW2 | 0.24 | 0.56 | 1.03 |

It can be seen in Table 7 that the torsional contribution of CFRP estimated by FIB-14 is generally unconservative. The third column of Table 7 shows the results obtained by average experimental effective strains and the FIB-14 method.

The nominal ultimate torsional strength of beams strengthened by FRP can be obtained through adding the contributions due to fibres to the torsional strength of the reinforced concrete beam with no FRP as follows:

$$T_n = T_{n_s} + T_{n_{frp}} \tag{8}$$

The equation for calculating the ultimate torsional strength of a reinforced concrete beam, recommended by ACI 318-05 [15] is

$$T_{n_s} = \frac{2A_o A_t f_{yv}}{s}\cot\alpha \tag{9}$$

where, $A_o$ is the cross-sectional area bounded by the centre line of the shear flow, $A_t$ is the area of one leg of the transverse steel reinforcement (stirrups) , $f_{yv}$ is the yield strength of the transverse steel reinforcement, and $s$ is the spacing of the stirrups.

Table 8 shows the comparison between experimental ultimate torsional strength and torsional strengths obtained from the analytical methods for all the strengthened beams.

Table 8. Comparison of experimental and analytical ultimate torques

| Specimen | $T_{exp}/T_n$ | $T_{exp}/T_n$ | $T_{exp}/T_n$ |
|---|---|---|---|
| | FIB-14 | Hii's method | FIB-14 & $\varepsilon_{f,\ ,exp}(\mu\varepsilon)$ |
| CS1 | 0.62 | 0.82 | 0.79 |
| CUJ-anc. | 0.60 | 0.91 | 0.98 |
| CW1 | 0.59 | 0.89 | 1.04 |
| CW2 | 0.43 | 0.75 | 1.10 |

A comparison of the results of the second and third methods demonstrates that the FIB-14 method, based upon the experimental effective strain, is more realistic. It is also found that the effective strain equations of FIB-14, using the effective strains values obtained from shear strengthening experiments, are not true. Therefore, new equations are necessary for calculating effective strain. These equations should be calibrated based on the statistical data obtained from torsional strengthening experiments.

## 4. CONCLUSION

From the analytical and experimental studies presented in this work, the following conclusions can be made:

1. The cracking and yield torques of all the strengthened beams are greater than the control beams. The increased magnitude depends on the CFRP's reinforcement ratio and the strengthening configuration. An increase of 48% in cracking and an increase of 32% in yield torque were recorded for beam CW2.
2. Adding anchors in the strengthening configuration of U-jacket wrapping is the reason that beam CUJ-anc. shows a torsional strength similar to that of beam CW1. This strengthening configuration (anchored FRP U-shape jacket) is important because it is practical and can be used in retrofitting T-shape beams which are simultaneously cast with the slabs.
3. Experimental results indicate that the estimation of the FRP contribution to torsional strength using the recommended equation in the literature is not true for beams strengthened by anchored U-shape wrapping. It is found that using the equation concerning full or strip wrapped specimens for such beams gives good results.
4. Comparing the ductility ratio based upon the post-peak phase of behavioural torque-twist curve to that of the beam without FRP shows that the ductility of beam CUJ-anc. is about 41% more than the ductility of beam CW1. Beam CUJ-anc. behaves better after post-peak, despite the fact that the top face of beam CUJ-anc. is not wrapped at all. In other words, unlike beam CW1, in beam CUJ-anc., the load decreases evenly after post-peak.
5. The largest ductility ratio among all the strengthened beams belongs to beam CW2, with an average value of 2.4 for two definitions of ductility ratio. This value shows about a 1.5 times increase in ductility compared to the average ductility of the control beams.
6. The torsional moment of the strengthened beams exceeded the torsional moment of the control beams by more than 75%. These results proved that composite materials will increase the torsional moment of RC beams significantly, even with minimum torsional reinforcement.
7. Comparing the results of the second and third methods of calculating FRP contribution demonstrates that using effective strain relationships of FIB-14 for estimating the torsional capacity of the retrofitted beams is viable. However, new equations are required to assess the effective strains based upon statistical data related to the experimental torsional strengthening.

***Acknowledgements***- The authors wish to express their sincere appreciation to the manager of ATIBAN Corporation, Mr. Shojaee, for his consistent support and for the facilities he provided.

## REFERENCES

1. Zhang, J. W., Lu, Z. T. & Zhu, H. (2001). Experimental study on the behaviour of RC torsional members externally bonded with CFRP. In: *FRP Composites in Civil Engineering*, Vol. 1, pp. 713-22.
2. Panchacharam, S. & Belarbi, A. (2002). Torsional behaviour of reinforced concrete beams strengthened with FRP composites. In: FIB Congress, Osaka Japan.
3. Ghobarah, A., Ghorbel, M. N. & Chidiac, S. E. (2002). Upgrading torsional resistance of reinforced concrete beams using fibre-reinforced polymer. *Journal of Composite for Construction*, Vol. 6, No. 4, pp. 257-63.
4. Gosbell, T. & Meggs, R. (2002). West Gate Bridge approach spans FRP strengthening Melbourne, Australia. In: *IABSE Symposium Melbourne*, Melbourne, Australia.
5. Ronagh, H. R. & Dux, P. F. (2003). Full-scale torsion testing of concrete beams strengthened with CFRP. In: *Proceedings of the First International Conference on the Performance of Construction Materials in the New Millenium*, February, Cairo, pp. 735-743.
6. Ameli, M., Ronagh, H. R. & Dux, P. F. (2004). Experimental investigations on FRP strengthening of beams in torsion. *FRP Composites in Civil Engineering-CICE 2004*, Adelaide, Australia, pp. 587-592.
7. Hii, A. K. Y. & Al-Mahaidi, R. (2004). Torsional strengthening of reinforced concrete beams using CFRP Composites. In: *FRP Composites in Civil Engineering - CICE 2004, Adelaide*, Australia, pp. 551-559.
8. Salom, P. R., Gergely, J. & Young, D. T. (2004). Torsional strengthening of spandrel beams with fibre-reinforced polymer laminates. *Journal of Composite for Construction*, Vol. 8, No. 2, pp. 157-162.
9. Hii, A. K. Y. & Al-Mahaidi, R. (2005). Torsional strengthening of solid and box-section RC beams using CFRP composites. *Composites in Construction 2005-Third International Conference*, Lyon, France, 59-68.
10. Hii, A. K. Y. & Al-Mahaidi, R. (2006). Experimental investigation on torsional behaviour of solid and box-section reinforced concrete beams strengthened with carbon FRP using photogrammetry. *Journal of Composite for Construction*, Vol. 10, No. 4, pp. 321-29.
11. Ameli, M., Ronagh, H. R. & Dux, P. F. (2007). Behaviour of FRP strengthened reinforced concrete beams under torsion. *Journal of Composite for Construction*, Vol. 11, No. 2, pp. 192-200.
12. Hii, A. K. Y. & Al-Mahaidi, R. (2007). Torsional capacity of CFRP strengthened reinforced concrete beams. *Journal of Composite for Construction*, Vol. 11, No. 1, pp. 71-80.
13. Mohammadizadeh, M. R. & Fadaee, M. J. (2009). Torsional behaviour of high-Strength concrete beams strengthened using CFRP sheets; an experimental and analytical Study. *International Journal of Science and Technology*, Vol. 16, No. 4, pp. 321-330.
14. Mohammadizadeh, M. R., Fadaee, M. J. & Ronagh, H. R. (2009). Improving torsional behaviour of reinforced concrete beams strengthened with carbon fibre reinforced polymer composite. *Iranian Polymer Journal*, Vol. 18, No. 4, pp. 315-327.
15. ACI 318-05, (2005). *Building code requirements for structural concrete*. American Concrete Institute.
16. Koutchoukali, N. & Belarbi, A. (2001). Torsion of high-strength reinforced concrete beams and minimum reinforcement requirements. *ACI Structural Journal*, Vol. 98, No. 4, pp. 462-69.
17. MBT, MBrace Brochure [online]; 2003. Available from: http://www.mbtaus.com.au.
18. Fang, I. K. & Shiau, J. K. (2004). Torsional behaviour of normal- and high-strength concrete beams. *ACI Structural Journal*, Vol. 101, No. 3, pp.304-13.

19. FIB. Externally bonded FRP reinforcement for RC structures, (2001). FIB Bulletin 14, FIB – International Federation for Structural Concrete, Lausanne, pp. 59-68.
20. Khalifa, A., Gold, W. J., Nanni, A. & Aziz, A. (1998). Contribution of externally bonded FRP to shear capacity of flexural members. *Journal of Composite for Construction*, Vol. 2, No. 4, pp. 195-203.